

Algorithm to design aperiodic optical superlattice for multiple quasi-phase matching

Ming Lu, Xianfeng Chen,* Yuping Chen, and Yuxing Xia

Department of Physics, the State Key Laboratory on Fiber Optic Local Area Communication Networks and Advanced Optical Communication Systems, Shanghai Jiao Tong University, 800 Dong Chuan Road, Shanghai 200240, China

*Corresponding author: xfchen@sjtu.edu.cn

Received 3 January 2007; accepted 9 March 2007;
posted 26 March 2007 (Doc. ID 78535); published 12 June 2007

We report a new algorithm, called the self-adjusting algorithm, to construct an aperiodic optical superlattice in which multiple nonlinear optical parametric processes can be realized simultaneously with high conversion efficiency. The numerical simulations show that a self-adjusting algorithm has obvious advantages that are due to its own physical process and feedback function. Especially in comparison with other existing algorithms, a self-adjusting algorithm can eliminate the need to search blindly and is independent of the initial conditions. © 2007 Optical Society of America

OCIS codes: 220.0220, 190.2620.

1. Introduction

Nonlinear crystal designs that exploit quasi-phase matching (QPM) can achieve considerable control over the wavelength conversion efficiency by modifying periods and structures of a nonlinear crystal [1]. With the development of room-temperature poling technology, it is possible to achieve domain-inverting structures in ferroelectric crystals such as LiNbO_3 , LiTaO_3 , and KTiOPO_4 [2–4]. The structures can be periodic or aperiodic [5]. From the theory of Fourier transformation, crystals with an aperiodic inverted-domain structure can supply more reciprocal vectors that can match more optical parametric processes simultaneously. As a trade-off, conversion efficiency of each parametric process would be lowered [6]. So, how to find the optimal optical superlattice for a given multiple optical parametric process is a key issue. Many methods have been proposed to solve the problem. Quasi-periodic optical superlattice (QOS), such as the fibonacci structure [7], was suggested. Quasi-phase-matched third-harmonic generation and multiple second-harmonic generation (SHG) have

been theoretically investigated [8–11]. Then came the theoretical prediction of the aperiodic optical superlattice (AOS) [12,13], which can supply many more reciprocal vectors for multiple QPM processes than a periodic optical superlattice and a QOS [14–17]. To find the optimal AOS structure, a simulated annealing (SA) algorithm, a genetic algorithm (GA), a genetic simulated annealing (GSA) algorithm (the combination of SA and GA) and other optimization algorithms were employed. However, all these optimization algorithms have the same disadvantages: the searching process is done blindly, so searching takes a long time, especially when dealing with a complicated problem. The searching process depends on initialization conditions and other parameters; the results are easy to incorporate into a local optimum, thus decreasing the conversion efficiency of the total multiple QPM process.

We suggest a new algorithm, which we refer to as a self-adjusting algorithm. The core concept of this algorithm is based on the procedure of energy flowing in QPM nonlinear optical processes, and a feedback function is introduced to avoid searching blindly. We proved that much better results can be found during a shorter calculation time when the optimized results can be kept from relapsing into

a local optimum. In addition, the process is independent of the initial conditions and other parameters.

2. Theory

As is known, to create a high-efficiency SHG, energy conservation and momentum conservation must be satisfied simultaneously. The AOS in LiNbO₃ crystal can be designed by use of a self-adjusting algorithm to satisfy multiple SHG conditions. In our calculations, the crystal with a total length L is divided into N unit blocks with congruent length ΔL , as shown in Fig. 1. The polarization direction of each block can be up or down, which is determined by the ensuing flows. To use the largest nonlinear coefficient d_{33} , let the interfaces of each domain be parallel to the Y - Z plane, and the propagation and the polarization directions of incident light are along the X and Z axes, respectively. Considering the small signal and the slowly varying approximation, the pump depletion and the transmission loss are also not taken into account. The conversion efficiency η from the fundamental wave to the SHG wave reads

$$\eta = \frac{8\pi^2 |d_{33}|^2 I_\omega L^2}{c \varepsilon_0 \lambda^2 n_{2\omega} n_\omega^2} \left| \frac{1}{L} \int_0^L d(z) e^{i\Delta k'(\lambda)z} dz \right|$$

[16], where $n_\omega(n_{2\omega})$ is the index of refraction of the fundamental (second harmonics) wave, c is the speed of light in vacuum, λ is the wavelength of the fundamental light in vacuum, ε_0 is the dielectric constant in vacuum, and $d(z)$ represents the orientation of each block taking binary values of 1 or -1 . We define the last term as an effective nonlinear optical coefficient

$$d_{\text{reff}}[\Delta k'(\lambda)] = \left| \frac{1}{L} \int_0^L d(z) e^{i\Delta k'(\lambda)z} dz \right|,$$

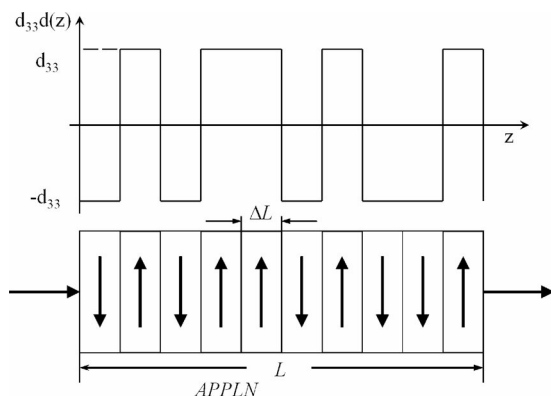


Fig. 1. Schematic of the periodic change of the nonlinear coefficient $d(z)$ along z . The arrowheads represent the polarization directions of positive or negative domains. Fundamental and second-harmonic wave propagation is along the Z direction.

which can scale the conversion efficiency of SHG by Fourier transformation. Here, $\Delta k'(\lambda) = k_{2\omega} - 2k_\omega$, where $k_\omega(k_{2\omega})$ is the wave vector of the fundamental (second harmonic) wave.

Thus, the original question turns into how to construct an AOS structure so that multiple high-efficiency QPM SHG processes can be made simultaneously, i.e., effective nonlinear coefficient $d_{\text{reff}}[\Delta k'(\lambda_i)]$ is optimal with identical value. Because the crystal is equally divided into N blocks, we have

$$\begin{aligned} d_{\text{reff}}[\Delta k'(\lambda)] &= \left| \frac{1}{L} \int_0^L d(z) e^{i\Delta k'(\lambda)z} dz \right| \\ &= \frac{1}{L} \left| \sum_{q=0}^{N-1} d(z_q) \int_{z_q}^{z_{q+1}} e^{i\Delta k'(\lambda)z} dz \right| \\ &= \frac{1}{L} \left| \sum_{q=0}^{N-1} d(z_q) \frac{e^{i\Delta k'(\lambda)z_{q+1}} - e^{i\Delta k'(\lambda)z_q}}{i\Delta k'(\lambda)} \right| \\ &= \frac{1}{L\Delta k'(\lambda)} \left| \sum_{q=0}^{N-1} d(z_q) (e^{i\Delta k'(\lambda)z_{q+1}} - e^{i\Delta k'(\lambda)z_q}) \right|. \end{aligned} \quad (1)$$

The phase mismatch can be described as

$$\Delta k'(\lambda) = k_{2\omega} - 2k_\omega = \frac{n_{2\omega} \cdot 2\omega}{c} - \frac{2n_\omega \cdot \omega}{c} = \frac{2\omega}{c} (n_{2\omega} - n_\omega). \quad (2)$$

A new vector $U_q(\lambda)$ is defined as $U_q(\lambda) = e^{i\Delta k'(\lambda)z_{q+1}} - e^{i\Delta k'(\lambda)z_q}$, which can be used to prove that, for a certain wavelength λ , $U_q(\lambda)$ is a group of N vectors with the same length because of the same length of each block ΔL , as shown in Fig. 2.

With the above definition, the effective nonlinear coefficient can be described as

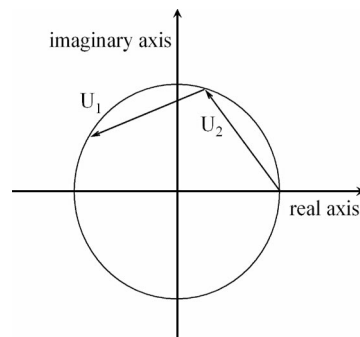


Fig. 2. Schematic diagram of $U_q(\lambda)$, which is a group of vectors with the same length and a specific direction; for example, $U_1(\lambda) = e^{i\Delta k'(\lambda)\Delta L}$ and $U_2(\lambda) = e^{i2\Delta k'(\lambda)\Delta L} - e^{i\Delta k'(\lambda)\Delta L}$.

$$d_{\text{reff}}[\Delta k'(\lambda)] = \frac{1}{L\Delta k'(\lambda)} \left| \sum_{q=0}^{N-1} d(z_q) U_q \right|. \quad (3)$$

As an example, to obtain the largest conversion efficiency for a specific wavelength λ , $d_{\text{reff}}[\Delta k'(\lambda)]$ should be maximum, i.e., $d(z_q)$ should be optimized by the algorithm so that

$$\left| \sum_{q=0}^{N-1} d(z_q) U_q \right|$$

is maximum and $1/[L\Delta k'(\lambda)]$ is constant for a given λ .

3. Example

As an example, we consider how to build an AOS based on LiNbO₃, which can achieve multiple SHG with an identical effective nonlinear coefficient, while SHG for other frequencies is considered as noise. The four chosen wavelengths of the fundamental wave are $\lambda_1 = 1060$ nm, $\lambda_2 = 1082$, $\lambda_3 = 1283$, $\lambda_4 = 1364$. Length L of the crystal is 9.9 mm, which is divided into 3000 unit blocks with congruent length ΔL and $\Delta L = 3.3$ μm . Based on the above theoretical analysis, the mathematical model has four groups of vectors: $\{U_q(\lambda_1)\}$, $\{U_q(\lambda_2)\}$, $\{U_q(\lambda_3)\}$, and $\{U_q(\lambda_4)\}$. $U_q(\lambda)$ is defined in Section 2, and $q = 3000$, so each $U_q(\lambda)$ has 3000 vectors with the same length, and their directions are determined by their $\Delta k'(\lambda) \cdot \Delta L$ and $d(z_q)$. The question is how to structure the optimal function $d(z_q)$ to obtain the absolute values of

$$\sum_q U_q(\lambda_1), \sum_q U_q(\lambda_2), \sum_q U_q(\lambda_3), \sum_q U_q(\lambda_4)$$

so they reach the same maximum value simultaneously. Generally, they are supposed to reach the same maximum value simultaneously with the specific angles of $\{\theta_1, \theta_2, \theta_3, \theta_4\}$, as shown in Fig. 3. In our calculations, we initially set these angles to be $\{0, 0, 0, 0\}$, which are parallel to the positive direction of the real axis. We will show that the selection of angles has only a slight influence on the optimized results. In this situation, the effective nonlinear coefficient for each specified wavelength can be described as

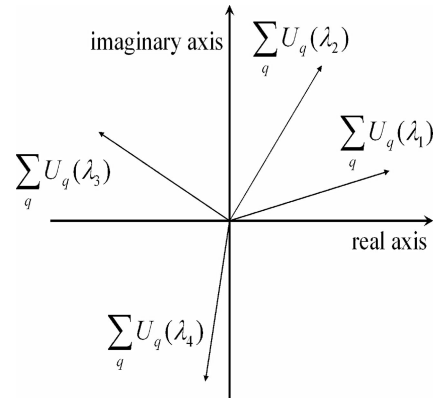


Fig. 3. Schematic diagram of the optimal result based on one specific function $d(z_q)$. $\sum_q U_q(\lambda_1)$, $\sum_q U_q(\lambda_2)$, $\sum_q U_q(\lambda_3)$, and $\sum_q U_q(\lambda_4)$ are supposed to reach the same maximum value simultaneously with specific angles $\{\theta_1, \theta_2, \theta_3, \theta_4\}$.

For each block, for example, the length from z_q to z_{q+1} , the contribution to the total $d_{\text{reff}}[\Delta k'(\lambda)]$, can be calculated as

$$d_{\text{reff}}(q) = \sum_{i=1}^4 \left[\frac{1}{L\Delta k'(\lambda_i)} \{ \cos[\Delta k'(\lambda_i)z_{q+1}] - \cos[\Delta k'(\lambda_i)z_q] \} \right]. \quad (5)$$

If $d_{\text{reff}}(q) \geq 0$, the value of $d(z_q)$ is set to 1 when $z \in (z_q, z_{q+1})$; if $d_{\text{reff}}(q) \leq 0$, the value of $d(z_q)$ is set to -1 when $z \in (z_q, z_{q+1})$. After calculating each block, the initialization of $d(z_q)$ is complete. In this AOS structure, the value of $\sum_{i=1}^4 d_{\text{reff}}[\Delta k'(\lambda_i)]$ is certain to be maximum. The calculation result is shown in Fig. 4(a). As can be seen, the values of $d_{\text{reff}}[\Delta k'(\lambda_1)]$, $d_{\text{reff}}[\Delta k'(\lambda_2)]$, $d_{\text{reff}}[\Delta k'(\lambda_3)]$, and $d_{\text{reff}}[\Delta k'(\lambda_4)]$ are 0.166, 0.187, 0.283, and 0.307, respectively, which are not equal to each other. The value of $\sum_{i=1}^4 d_{\text{reff}}[\Delta k'(\lambda_i)]$ is 0.943.

To average four $d_{\text{reff}}[\Delta k'(\lambda)]$, new function $R(r_1, r_2, r_3, r_4)$ is introduced to change the weight of these four frequencies that supports the feedback function. The result is that the sum of four $d_{\text{reff}}[\Delta k'(\lambda_i)]$ can be lowered to some degree. When $R(r_1, r_2, r_3, r_4)$ is not introduced, it can be regarded as $(1, 1, 1, 1)$. For the first optimizing step, $R(r_1, r_2, r_3, r_4)$ is reset to

$$\begin{aligned} d_{\text{reff}}[\Delta k'(\lambda_1)] &= \frac{1}{L\Delta k'(\lambda_1)} \left(\sum_{q=0}^{N-1} d(z_q) \{ \cos[\Delta k'(\lambda_1)z_{q+1}] - \cos[\Delta k'(\lambda_1)z_q] \} \right), \\ d_{\text{reff}}[\Delta k'(\lambda_2)] &= \frac{1}{L\Delta k'(\lambda_2)} \left(\sum_{q=0}^{N-1} d(z_q) \{ \cos[\Delta k'(\lambda_2)z_{q+1}] - \cos[\Delta k'(\lambda_2)z_q] \} \right), \\ d_{\text{reff}}[\Delta k'(\lambda_3)] &= \frac{1}{L\Delta k'(\lambda_3)} \left(\sum_{q=0}^{N-1} d(z_q) \{ \cos[\Delta k'(\lambda_3)z_{q+1}] - \cos[\Delta k'(\lambda_3)z_q] \} \right), \\ d_{\text{reff}}[\Delta k'(\lambda_4)] &= \frac{1}{L\Delta k'(\lambda_4)} \left(\sum_{q=0}^{N-1} d(z_q) \{ \cos[\Delta k'(\lambda_4)z_{q+1}] - \cos[\Delta k'(\lambda_4)z_q] \} \right). \end{aligned} \quad (4)$$

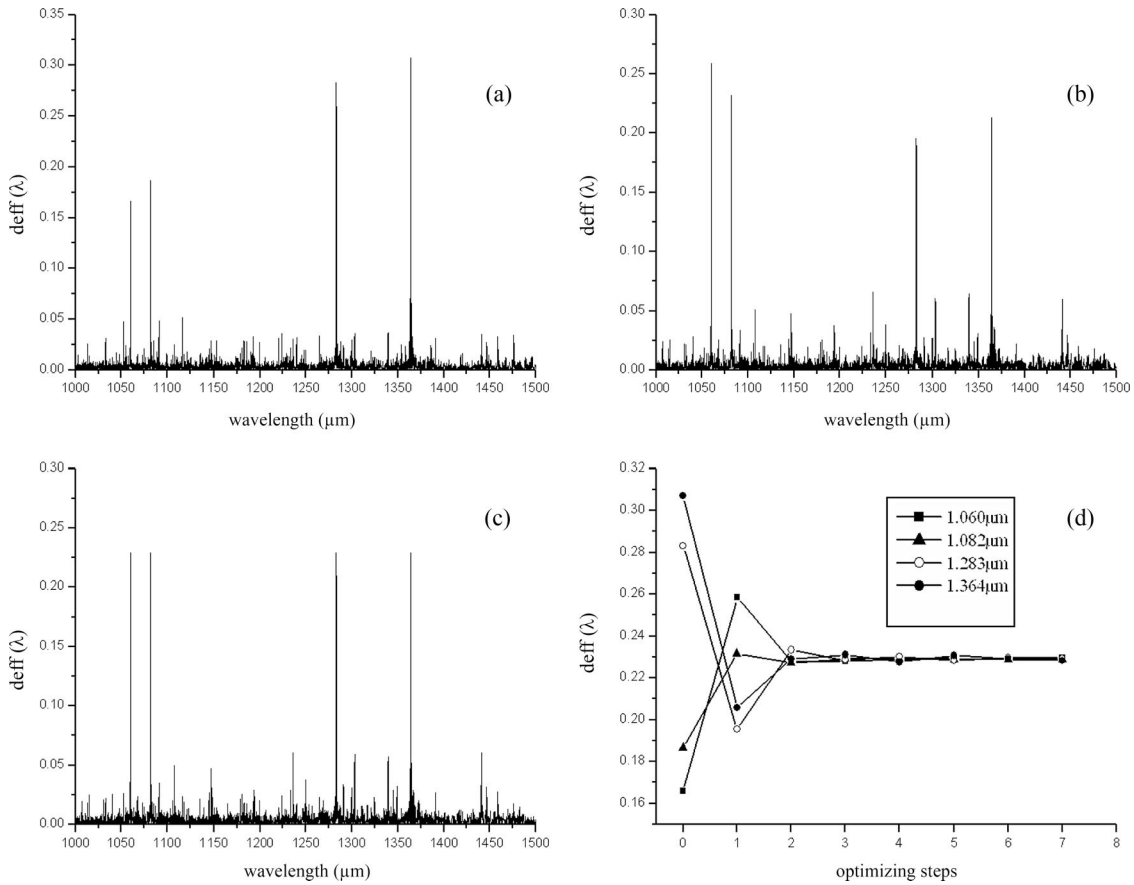


Fig. 4. (a) Result without introducing $R(r_1, r_2, r_3, r_4)$, (b) result after one optimizing step, (c) the result after seven optimizing step. (d) The four peak values at the designed wavelength after each optimization step. After three steps, the four peak values are close to each other. After seven steps, four peaks with identical effective nonlinear coefficients of 0.229 at the designed wavelengths are determined. Effective nonlinear coefficient of QPM SHG as a function of fundamental wavelength in the AOS structure optimized by the self-adjusting algorithm with $N = 3000$ and $\Delta L = 3.3 \mu\text{m}$. The designed wavelengths are 1060, 1082, 1283, and 1364 nm.

$$\left(\frac{1}{0.166}, \frac{1}{0.187}, \frac{1}{0.283}, \frac{1}{0.307} \right).$$

This time the algorithm seeks the maximum of $\sum_{i=1}^4 r_i d_{\text{reff}}[\Delta k'(\lambda_i)]$ instead of $\sum_{i=1}^4 d_{\text{reff}}[\Delta k'(\lambda_i)]$. After this step, a new AOS structure is obtained, and the values of the four peaks are 0.258, 0.232, 0.196, 0.206, as shown in Fig. 4(b). The second optimizing step is to adjust the above $R(r_1, r_2, r_3, r_4)$ to be

$$\left(\frac{r_1}{0.258}, \frac{r_2}{0.232}, \frac{r_3}{0.196}, \frac{r_4}{0.206} \right)$$

and then search for a new AOS structure that satisfies the maximum of $\sum_{i=1}^4 r_i d_{\text{reff}}[\Delta k'(\lambda_i)]$. After seven optimizing steps, values of $d_{\text{reff}}[\Delta k'(\lambda_1)]$, $d_{\text{reff}}[\Delta k'(\lambda_2)]$, $d_{\text{reff}}[\Delta k'(\lambda_3)]$, and $d_{\text{reff}}[\Delta k'(\lambda_4)]$ are all 0.229, as shown in Fig. 4(c). $\sum_{i=1}^4 d_{\text{reff}}[\Delta k'(\lambda_i)]$ is 0.916, which is quite close to the ultimate value of 0.943. So the depletion generated by $R(r_1, r_2, r_3, r_4)$ is small. The value of $R(r_1, r_2, r_3, r_4)$ is (39889, 36562, 25621, 24073). The computation time is within 1 s, which is much shorter than the time computed by other algorithms. The

optimized results after each step are shown in Fig. 4(d). In addition, we can also achieve the peaks by any arbitrary proportion we want by setting different $R(r_1, r_2, r_3, r_4)$.

Figure 5 describes the evolution of the effective nonlinear coefficient of four fundamental waves as they propagate through a series of domain blocks in the AOS. Figure 5 shows that each curve moves to the same end point in different ways. This clearly shows that these wavelengths can all be globally phase matched by the interference effect of all the constructed domains with the same effective nonlinear coefficient, but they undergo different interference processes. For convenience, we set the angles $\{\theta_1, \theta_2, \theta_3, \theta_4\}$ to be (0, 0, 0, 0). When we change the angles $\{\theta_1, \theta_2, \theta_3, \theta_4\}$ arbitrarily, the peaks change only slightly.

4. Analysis

Compared with other algorithms, such as SA, GA, and GSA, the combination of SA and GA, the advantages of the self-adjusting algorithm are obvious. The SA method specializes in yielding the best local results but is not good at searching the overall space. The GA method can easily be used to guide the search

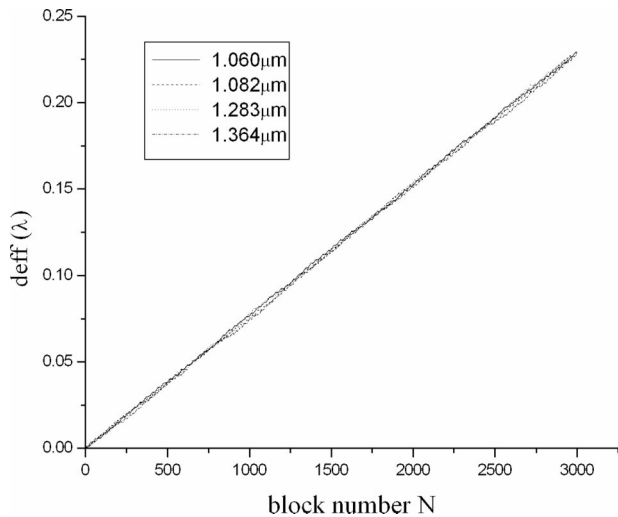


Fig. 5. Display of the SHG effective nonlinear coefficient of four fundamental wavelengths as they propagate in the AOS sample. The four SHG efficiencies of four wavelengths reach one identical value at the end.

process to the correct direction, but the GA cannot get the best local results with high efficiency. The computational amount of both the GA and the SA is usually huge and requires quite a long time to solve the problem. The GSA algorithm takes advantage of both the SA and the GA and has proved to be an excellent algorithm. The optimization result of a nonlinear optical superlattice in LiNbO_3 from the GSA algorithm has been reported [12] with the same length of crystal and the same number of blocks when dealing with the same multiple SHG problem. The value of each $d_{\text{reff}}[\Delta k'(\lambda_i)]$ is approximately 0.14, much lower than the result of the self-adjusting algorithm, whereas the noise is much higher. The calculation time takes approximately 8 h, the calculation time for the self-adjusting algorithm is less than 1 s.

The main idea of the self-adjusting algorithm is similar to the A+ heuristic algorithm and also takes the feedback function into consideration. Compared with other existing algorithms, the self-adjusting algorithm has significant advantages.

First, the self-adjusting algorithm is based on a specific nonlinear optical process, such as multiple QPM SHG or other frequency conversion processes that take into account the real situation and physical principle when optimizing the structure; other algorithms do not consider the actual physical process. The self-adjusting algorithm can also be used to solve other optical parametric processes, such as optical parametric oscillation, different frequency mixing, only by changing some specific parameters.

Second, the self-adjusting algorithm uses a feedback function to avoid searching blindly, so the calculation time is much shorter. Other algorithms are based on macroscopic computation, the searching processes for optimal results are done blindly and require huge amounts of calculation as well as repet-

itive huge amounts of tentative calculations. So, the self-adjusting algorithm has a significant advantage when dealing with more complicated QPM optimization questions.

Third, the self-adjusting algorithm is independent of initial conditions. The results gained by other algorithms depend on their initial conditions, which could lead to different solutions. To confirm a most suitable initial condition is usually difficult. For the self-adjusting algorithm, the definition of $R(r_1, r_2, r_3, r_4)$ is an analog to the initial condition. Usually, $R(r_1, r_2, r_3, r_4)$ is defined as (1, 1, 1, 1). Actually, the arbitrary initial value of $R(r_1, r_2, r_3, r_4)$ could approach the same optimized results.

Last but not least, when using other algorithms, such as SA, GA, and GSA, some specialized parameters need to be confirmed. For example, population size, mating rule, and fitness function for the GA; initial temperature and annealing speed for the SA. If one of these parameters is not suitable, the searching results could be unsatisfactory. Besides, confirmation of parameters is a difficult mission. The self-adjusting algorithm has nothing to do with these parameters, which is a great convenience for the designer.

5. Conclusion

In summary, we have proposed a new algorithm to search for the ideal construction of an AOS that corresponds to a frequency conversion problem. The calculated results show that it is more flexible and effective than other existing algorithms. By using this algorithm, we can construct the AOS with a higher conversion efficiency. It can also be used to solve other optimization problems with different optical parametric processes.

This research was supported by the National Natural Science Foundation of China (60477016 and 10574092), the Foundation for Development of Science and Technology of Shanghai (04DZ14001), and the Shu-Guang Scholar Plan of the Shanghai Education Committee.

References

1. A. Armstrong, N. Bloembergen, J. Ducuing, and P. S. Pershan, "Interactions between light waves in a nonlinear dielectric," *Phys. Rev.* **127**, 1918–1939 (1962).
2. J. C. Peuzin, "Comment on Domain inversion effects in Ti–LiNbO₃ integrated optical devices," *Appl. Phys. Lett.* **48**, 1104 (1986).
3. S. Miyazawa, "Response to Comment on Domain inversion effects in Ti–LiNbO₃ integrated optical devices," *Appl. Phys. Lett.* **48**, 1105 (1986).
4. M. Yamada, N. Nada, M. Saitoh, and K. Watanabe, "First-order quasi-phase matched LiNbO₃ waveguide periodically poled by applying an external field for efficient blue second-harmonic generation," *Appl. Phys. Lett.* **62**, 435–436 (1993).
5. S. N. Zhu, Y. Y. Zhu, and N. B. Ming, "Quasi-phase-matched third-harmonic generation in a quasi-periodic optical superlattice," *Science* **278**, 843–846 (1997).
6. K. Mizuuchi, T. Sugita, K. Yamamoto, T. Kawaguchi, T. Yoshino, and M. Imaeda, "Efficient 340 nm light generation by a

- ridge-type waveguide in a first-order periodically poled MgO:LiNbO₃,” *Opt. Lett.* **28**, 1344–1346 (2003).
7. S. N. Zhu, Y. Y. Zhu, Y. Q. Qin, H. F. Wang, C. Z. Ge, and N. B. Ming, “Experimental realization of second harmonic generation in a fibonacci optical superlattice of LiTaO₃,” *Phys. Rev. Lett.* **78**, 2752–2755 (1997).
 8. B. Y. Gu, B. Z. Dong, Y. Zhang, and G. Z. Yang, “Enhanced harmonic generation in aperiodic optical superlattices,” *Appl. Phys. Lett.* **75**, 2175–2177 (1999).
 9. B. Y. Gu, Y. Zhang, B. Z. Dong, “Investigations of harmonic generations in aperiodic optical superlattices,” *J. Appl. Phys.* **87**, 7629–7637 (2000).
 10. Y. Zhang and B. Y. Gu, “Optimal design of aperiodically poled lithium niobate crystals for multiple wavelengths parametric amplification,” *Opt. Commun.* **192**, 417–425 (2001).
 11. A. H. Norton and C. M. de Sterke, “Aperiodic 1-dimensional structures for quasi-phase matching,” *Opt. Express* **12**, 841–846 (2004).
 12. X. Chen, F. Wu, X. Zeng, Y. Chen, Y. Xia, and Y. Chen, “Multiple quasi-phase-matching in a nonperiodic domain-inverted optical superlattice,” *Phys. Rev. A* **69**, 013818 (2004).
 13. X. L. Zeng, X. F. Chen, F. Wu, Y. P. Chen, Y. X. Xia, and Y. L. Chen, “Second-harmonic generation with broadened flat-top bandwidth in aperiodic domain-inverted gratings,” *Opt. Commun.* **204**, 407–411 (2002).
 14. P. A. Franken and J. F. Ward, “Optical harmonics and nonlinear phenomena,” *Rev. Mod. Phys.* **35**, 23–39 (1963).
 15. S. Matsumoto, E. J. Lim, H. M. Hertz, and M. M. Fejer, “Quasiphase-matched second harmonic generation of blue light in electrically periodically-poled lithium tantalate waveguides,” *Electron. Lett.* **27**, 2040–2042 (1991).
 16. N. Bloembergen and A. J. Sievers, “Nonlinear optical properties of periodic laminar structures,” *Appl. Phys. Lett.* **17**, 483–486 (1970).
 17. G. D. Miller, R. G. Batchko, W. M. Tulloch, D. R. Weise, M. M. Fejer, and R. L. Byer, “42%-efficient single-pass cw second-harmonic generation in periodically poled lithium niobate,” *Opt. Lett.* **22**, 1834–1836 (1997).